

Functional Tucker approximation using Chebyshev interpolation

Sergey Dolgov¹, Daniel Kressner², and Christoph Strössner³

¹Department of Mathematical Sciences, University of Bath, United Kingdom,
S.Dolgov@bath.ac.uk

²Institute of Mathematics, EPF Lausanne, Switzerland, daniel.kressner@epfl.ch.

³Institute of Mathematics, EPF Lausanne, Switzerland, christoph.stroessner@epfl.ch.

July 31, 2020

Abstract

This work is concerned with approximating a trivariate function defined on a tensor-product domain via function evaluations. Combining tensorized Chebyshev interpolation with a Tucker decomposition of low multilinear rank yields function approximations that can be computed and stored very efficiently. The existing Chebfun3 algorithm [Hashemi and Trefethen, *SIAM J. Sci. Comput.*, 39 (2017)] uses a similar format but the construction of the approximation proceeds indirectly, via a so called slice-Tucker decomposition. As a consequence, Chebfun3 sometimes uses unnecessarily many function evaluation and does not fully benefit from the potential of the Tucker decomposition to reduce, sometimes dramatically, the computational cost. We propose a novel algorithm Chebfun3F that utilizes univariate fibers instead of bivariate slices to construct the Tucker decomposition. Chebfun3F reduces the cost for the approximation for nearly all functions considered, typically by 75%, and sometimes by over 98%.

1 Introduction

This work is concerned with the approximation of trivariate functions (that is, functions depending on three variables) defined on a tensor-product domain, for the purpose of performing numerical computations with these functions. Standard approximation techniques, such as interpolation on a regular grid, may require an impractical amount of function evaluations. Several techniques have been proposed to reduce the number of evaluations for multivariate functions by exploiting additional properties. For example, sparse grid interpolation [8] exploits mixed regularity. Alternatively, functional low-rank (tensor) decompositions, such as the spectral tensor train decomposition [6], the continuous low-rank decomposition [22, 23], and the QTT decomposition [31, 41], have been proposed. In this work, we focus on using the Tucker decomposition for third-order tensors, following work by Hashemi and Trefethen [29].

The original problem of finding separable decompositions of functions is intimately connected to low-rank decompositions of matrices and tensors [25, Chapter 7]. A trivariate function is called separable if it can be represented as a product of univariate functions: $f(x, y, z) = u(x)v(y)w(z)$. If such a decomposition is available, it is usually much more efficient to work with the factors u, v, w instead of f when, e.g., discretizing the function. In practice, most functions are usually not separable, but they often can be well approximated by a sum of separable functions. Additional structure can be imposed on this sum, corresponding to different tensor formats. In this work, we consider the approximation of a function $f : [-1, 1]^3 \rightarrow \mathbb{R}$ in the functional Tucker format [56], as in [29, 35, 44], which takes the form

$$f(x, y, z) \approx \sum_{i=1}^{r_1} \sum_{j=1}^{r_2} \sum_{k=1}^{r_3} c_{ijk} u_i(x) v_j(y) w_k(z), \quad (1)$$

with univariate functions $u_i, v_j, w_k: [-1, 1] \rightarrow \mathbb{R}$ and the so called *core tensor* $\mathcal{C} \in \mathbb{R}^{r_1 \times r_2 \times r_3}$. The minimal $r = (r_1, r_2, r_3)$, for which (1) can be satisfied with equality is called multilinear rank of f . It determines the number of entries in \mathcal{C} and the number of univariate functions needed to represent f . For functions depending on more than three variables, a recursive format is usually preferable, leading to tree based formats [20, 38, 39] such as the hierarchical Tucker format [28, 49] and the tensor train format [42, 6, 16, 22, 23].

The existence of a good approximation of the form (1) depends, in a nontrivial manner, on properties of f . It can be shown that the best approximation error in the format decays algebraically with respect to the multilinear rank of the approximation for functions in Sobolev Spaces [24, 49] and geometrically for analytic functions [27, 55]. Approximations based on the Tucker format are highly anisotropic [54], i.e., a rotation of the function may lead to a very different behavior of the approximation error. This can be partially overcome by adaptively subdividing the domain of the function as proposed, e.g., by Aiton and Driscoll [1].

The representation (1) is not yet practical because it involves continuous objects; a combination of low-rank tensor *and* function approximation is needed. Univariate functions can be approximated using barycentric Lagrange interpolation based on Chebyshev points [2, 5, 30]. This interpolation is fundamental to Chebfun [19] - a package providing tools to perform numerical computations on the level of functions [43]. Operations with these functions are internally performed by manipulating the Chebyshev coefficients of the interpolant [3].

In Chebfun2 [51, 52], a bivariate function $f(x, y)$ is approximated by applying Adaptive Cross Approximation (ACA) [4], which yields a low-rank approximation in terms of function fibers (e.g. $f(x_*, y)$ for fixed x_* but varying y), and interpolating these fibers. In Chebfun3, Hashemi and Trefethen [29] extended these ideas to trivariate functions by recursively applying ACA, to first break down the tensor to function slices (e.g., $f(x_*, y, z)$ for fixed x_*) and then to function fibers. As will be explained in Section 3.4, this indirect approach via slice approximations typically leads to redundant function fibers, which in turn involve unnecessary function evaluations. This is particularly problematic when the evaluation of the function is expensive, e.g. when each sample requires the solution of a partial differential equation (PDE); see Section 5 for an example.

In this paper, we propose a novel algorithm aiming at computing the Tucker decomposition directly. Our algorithm is called Chebfun3F to emphasize that it is based on selecting the *Fibers* u_i, v_j, w_k in the Tucker approximation (1). To compute a suitable core tensor, oblique projections based on Discrete Empirical Interpolation (DEIM) [11] are used. We combine this approach with heuristics similar to the ones used in Chebfun3 for choosing the univariate discretization parameters adaptively and for the accuracy verification.

The remainder of this paper is structured as follows. In Section 2, we introduce and analyze the approximation format used in Chebfun3 and Chebfun3F. In Section 3, we briefly recall the approximation algorithm currently used in Chebfun3. Section 4 introduces our novel algorithm Chebfun3F. Finally, in Section 5, we perform numerical experiments to compare Chebfun3, Chebfun3F and sparse grid interpolation.

2 Chebyshev Interpolation and Tucker Approximation

2.1 Chebyshev Interpolation

Given a function $f: [-1, 1]^3 \rightarrow \mathbb{R}$, we consider an approximation of the form

$$f(x, y, z) \approx \tilde{f}(x, y, z) = \sum_{i=1}^{n_1} \sum_{j=1}^{n_2} \sum_{k=1}^{n_3} \mathcal{A}_{ijk} T_i(x) T_j(y) T_k(z), \quad (2)$$

where $\mathcal{A} \in \mathbb{R}^{n_1 \times n_2 \times n_3}$ is the coefficient tensor and $T_k(x) = \cos(k \cos^{-1}(x))$ denotes the k -th Chebyshev polynomial.

To construct (2), we use (tensorized) interpolation. Let $\mathcal{T}_{ijk} = f(x_i^{(1)}, x_j^{(2)}, x_k^{(3)})$ denote the tensor containing all function values on the grid of Chebyshev points $x_k^{(\alpha)} = \cos(k\pi/(n_\alpha - 1))$, $k = 1, \dots, n_\alpha$ [53]. The coefficient tensor \mathcal{A} is computed from \mathcal{T} using Fourier transformations. We define the transformation

matrices $F^{(\alpha)} \in \mathbb{R}^{n_\alpha \times n_\alpha}$ for $\alpha = 1, 2, 3$ as in [36, Sec. 8.3.2.]

$$F_{ij}^{(\alpha)} = \frac{2}{n_\alpha} \begin{pmatrix} \frac{1}{4}T_0(x_0^{(\alpha)}) & \frac{1}{2}T_0(x_1^{(\alpha)}) & \frac{1}{2}T_0(x_2^{(\alpha)}) & \dots & \frac{1}{4}T_0(x_{n_\alpha}^{(\alpha)}) \\ \frac{1}{2}T_1(x_0^{(\alpha)}) & T_1(x_1^{(\alpha)}) & T_1(x_0^{(\alpha)}) & \dots & \frac{1}{2}T_1(x_{n_\alpha}^{(\alpha)}) \\ \frac{1}{2}T_2(x_0^{(\alpha)}) & T_2(x_1^{(\alpha)}) & T_2(x_0^{(\alpha)}) & \dots & \frac{1}{2}T_2(x_{n_\alpha}^{(\alpha)}) \\ \vdots & \vdots & \vdots & \ddots & \vdots \\ \frac{1}{4}T_{n_\alpha}(x_0^{(\alpha)}) & \frac{1}{2}T_{n_\alpha}(x_1^{(\alpha)}) & \frac{1}{2}T_{n_\alpha}(x_2^{(\alpha)}) & \dots & \frac{1}{4}T_{n_\alpha}(x_{n_\alpha}^{(\alpha)}) \end{pmatrix}.$$

The mapping from the function evaluations to the coefficients can now be written as

$$\mathcal{A} = \mathcal{T} \times_1 F^{(1)} \times_2 F^{(2)} \times_3 F^{(3)}, \quad (3)$$

where $\mathcal{T} \times_\alpha M$ denotes the mode- α multiplication. For a tensor $\mathcal{T} \in \mathbb{R}^{n_1 \times n_2 \times n_3}$ and a matrix $M \in \mathbb{R}^{m \times n_\alpha}$ it is defined as the multiplication of every mode- α fiber of \mathcal{T} with M , i.e.

$$(\mathcal{T} \times_\alpha M)^{\{\alpha\}} = M\mathcal{T}^{\{\alpha\}},$$

where $\mathcal{T}^{\{\alpha\}}$ denotes the mode- α matricization, which is the matrix containing all mode- α fibers of \mathcal{T} [33]. By construction, the interpolation condition $\tilde{f}(x_i^{(1)}, x_j^{(2)}, x_k^{(3)}) = f(x_i^{(1)}, x_j^{(2)}, x_k^{(3)})$ is satisfied in all Chebyshev points.

The approximation error for Chebyshev interpolation applied to multivariate analytic functions has been studied, e.g., by Sauter and Schwab in [47]. The following result states that the error decays exponentially with respect to the number of interpolation points in each variable.

Theorem 1 ([47, Lemma 7.3.3.]). *Suppose that $f \in C([-1, 1]^3)$ can be extended to an analytic function f^* on $\mathcal{E}_\rho = E_{\rho_1} \times E_{\rho_2} \times E_{\rho_3}$ with $\rho_i > 1$, where E_ρ denotes the Bernstein ellipse, a closed ellipse with foci at ± 1 and the sum of major and minor semi-axes equal to ρ . Then the Chebyshev interpolant \tilde{f} constructed above satisfies for $n = n_1 = n_2 = n_3$ the error bound*

$$\|f - \tilde{f}\|_\infty \leq 2^{2.5} \sqrt{3} \rho_{\min}^{-n} (1 - \rho_{\min}^{-2})^{1.5} \max_{z \in \mathcal{E}_\rho} |f^*(z)|,$$

where $\|\cdot\|_\infty$ denotes the uniform norm on $[-1, 1]^3$ and $\rho_{\min} = \min(\rho_1, \rho_2, \rho_3)$.

2.2 Tucker Approximations

A Tucker approximation of multilinear rank (r_1, r_2, r_3) for a tensor $\mathcal{T} \in \mathbb{R}^{n_1 \times n_2 \times n_3}$ takes the form

$$\mathcal{T} \approx \hat{\mathcal{T}} = \mathcal{C} \times_1 U \times_2 V \times_3 W,$$

where $\mathcal{C} \in \mathbb{R}^{r_1 \times r_2 \times r_3}$ is called core tensor and $U \in \mathbb{R}^{n_1 \times r_1}$, $V \in \mathbb{R}^{n_2 \times r_2}$, $W \in \mathbb{R}^{n_3 \times r_3}$ are called factor matrices. If $r_\alpha \ll n_\alpha$, the required storage is reduced from $n_1 n_2 n_3$ for \mathcal{T} to $r_1 r_2 r_3 + r_1 n_1 + r_2 n_2 + r_3 n_3$ for $\hat{\mathcal{T}}$.

2.3 Combining the Tucker Approximation and Chebyshev Interpolation

Let $\hat{\mathcal{T}} = \mathcal{C} \times_1 U \times_2 V \times_3 W$ be a Tucker approximation of the tensor \mathcal{T} obtained from evaluating f in Chebyshev points. Inserted into (2), we now consider an approximation of the form

$$\hat{f}(x, y, z) = \sum_{i=1}^{n_1} \sum_{j=1}^{n_2} \sum_{k=1}^{n_3} \hat{\mathcal{A}}_{ijk} T_i(x) T_j(y) T_k(z), \quad (4)$$

where the interpolation coefficients $\hat{\mathcal{A}}$ are computed from $\hat{\mathcal{T}}$ as in Equation (3)

$$\begin{aligned}\hat{\mathcal{A}} &= \hat{\mathcal{T}} \times_1 F^{(1)} \times_2 F^{(2)} \times_3 F^{(3)} \\ &= \mathcal{C} \times_1 F^{(1)}U \times_2 F^{(2)}V \times_3 F^{(3)}W.\end{aligned}$$

Note that the application of $F^{(\alpha)}$ is the mapping from function evaluations to interpolation coefficients in the context of univariate Chebyshev interpolation [3, 36]. By interpreting the values stored in the columns of U as function evaluations at Chebyshev points, we can define its columnwise Chebyshev interpolant $U(x) = [u_1(x), \dots, u_{r_1}(x)]$, where $u_j(x) = \sum_{i=1}^{n_1} (F^{(1)}U)_{ij} T_i(x)$. Note that $U(x) \in \mathbb{R}^{1 \times r_1}$ for fixed x . Defining $V(y)$ and $W(z)$ analogously allows us to rewrite the approximation (4) as

$$\hat{f}(x, y, z) = \mathcal{C} \times_1 U(x) \times_2 V(y) \times_3 W(z), \quad (5)$$

where the mode- α products are defined as in Section 2.1 for fixed x, y, z . The goal of this paper is to compute approximations of this form.

2.4 Low-Rank Approximation Error

The following lemma allows us to distinguish the interpolation error from the low-rank approximation error in the approximation (5).

Lemma 1. *Consider the Chebyshev interpolation \tilde{f} defined in (2) and let $\hat{\mathcal{T}}$ be an approximation of the involved function evaluation tensor $\mathcal{T} \in \mathbb{R}^{n_1 \times n_2 \times n_3}$. Then the approximation \hat{f} defined in (5) satisfies*

$$\|f - \hat{f}\|_\infty \leq \|f - \tilde{f}\|_\infty + \left(\frac{2}{\pi} \log(n_1) + 1\right) \left(\frac{2}{\pi} \log(n_2) + 1\right) \left(\frac{2}{\pi} \log(n_3) + 1\right) \|\mathcal{T} - \hat{\mathcal{T}}\|_\infty. \quad (6)$$

Proof. By applying the triangle inequality we obtain

$$\|f - \hat{f}\|_\infty \leq \|f - \tilde{f}\|_\infty + \|\tilde{f} - \hat{f}\|_\infty.$$

Tensorized interpolation is equivalent to applying univariate interpolation to each mode. The operator norm for univariate interpolation in m Chebyshev points, the Lebesgue constant, satisfies $\Lambda_m \leq (2/\pi) \log(m) + 1$ [53]. Because interpolation is a linear operation, we obtain

$$\|\tilde{f} - \hat{f}\|_\infty \leq \Lambda_{n_1} \Lambda_{n_2} \Lambda_{n_3} \|\mathcal{T} - \hat{\mathcal{T}}\|_\infty \leq \left(\frac{2}{\pi} \log(n_1) + 1\right) \left(\frac{2}{\pi} \log(n_2) + 1\right) \left(\frac{2}{\pi} \log(n_3) + 1\right) \|\mathcal{T} - \hat{\mathcal{T}}\|_\infty.$$

□

Lemma 1 states that \hat{f} is nearly as accurate as \tilde{f} when the error bound (6) is not dominated by $\|\mathcal{T} - \hat{\mathcal{T}}\|_\infty$. The low-rank approximation \hat{f} can be stored more efficiently than \tilde{f} when $r_\alpha \ll n_\alpha$. In the next section, we provide some insight into an example that features $r_\alpha \ll n_\alpha$.

2.5 When the Low-Rank Approximation is More Accurate

We consider the function

$$f_\varepsilon(x, y, z) = \frac{1}{x + y + z + 3 + \varepsilon}$$

on $[-1, 1]^3$ with parameter $\varepsilon > 0$. Let $\tau \geq 0$.

In this section, we show that a Chebyshev interpolation \tilde{f}_ε satisfying $\|\tilde{f}_\varepsilon - f_\varepsilon\|_\infty \leq \tau$ for a prescribed error bound τ requires polynomial degrees $n_\alpha = \mathcal{O}(1/\log(1 + \sqrt{\varepsilon}))$, which grows algebraically in $1/\varepsilon$. However, one can achieve $\|\mathcal{T} - \hat{\mathcal{T}}\|_\infty \leq \tau$ with multilinear ranks $r_\alpha \leq \mathcal{O}(|\log(\varepsilon)|)$. Therefore for small values of ε the required polynomial degree is much higher than the required multilinear rank. In this situation \hat{f}_ε can achieve almost the same accuracy as \tilde{f}_ε , but with significantly less storage.

Polynomial Degree

For the degree (n_1, n_2, n_3) Chebyshev interpolant \tilde{f}_ε we require $\|f_\varepsilon - \tilde{f}_\varepsilon\|_\infty \leq \tau$, which is equivalent to $\|\varepsilon(f_\varepsilon - \tilde{f}_\varepsilon)\|_\infty \leq \varepsilon\tau$. By Theorem 1,

$$\|\varepsilon(f_\varepsilon - \tilde{f}_\varepsilon)\|_\infty \leq \mathcal{O}(\rho_{\min}^{-n} \cdot \max_{z \in \mathcal{E}_\rho} |\varepsilon f_\varepsilon^*(z)|).$$

We set $\rho_1 = \rho_2 = \rho_3 = 1 + \varepsilon/6 + \sqrt{(1 + \varepsilon/6)^2 - 1}$ and extend $\varepsilon f_\varepsilon$ analytically to $\varepsilon f_\varepsilon^*(x, y, z) = \varepsilon(x + y + z + 3 + \varepsilon)^{-1}$ on \mathcal{E}_ρ . By construction $\max_{z \in \mathcal{E}_\rho} |\varepsilon f_\varepsilon^*(z)| = 2$. Hence, we can choose $n_1 = n_2 = n_3 = \mathcal{O}(1/\log(1 + \sqrt{\varepsilon}))$ to obtain the desired accuracy. Although this is only an upper bound for the polynomial degree required, numerical experiments reported below indicate that it is tight.

Multilinear Rank

An a priori approximation with exponential sums is used to obtain a bound on the multilinear rank for a tensor containing function values of f_ε ; see [26]. Given $R > 1$ and $r \in \mathbb{N}$, Braess and Hackbusch [7] showed that there exist coefficients a_i and b_i such that

$$\left| \frac{1}{x} - \sum_{i=1}^r a_i \exp(-b_i x) \right| \leq 16 \exp\left(-\frac{r\pi^2}{\log(8R)}\right), \quad \forall x \in [1, R]. \quad (7)$$

Trivially, we have $\varepsilon f_\varepsilon(x, y, z) = 1/\omega$ for the substitution $\omega = (x + y + z + 3 + \varepsilon)/\varepsilon$ with $\omega \in [1, 1 + 6/\varepsilon]$. Applying (7) yields $|1/\omega - s_r(\omega)| \leq \tau\varepsilon$ or, equivalently,

$$\left\| f_\varepsilon(x, y, z) - \underbrace{\sum_{i=1}^r \frac{a_i}{\varepsilon} \cdot \exp\left(-\frac{b_i}{\varepsilon} x\right) \cdot \exp\left(-\frac{b_i}{\varepsilon} y\right) \cdot \exp\left(-\frac{b_i}{\varepsilon} z\right) \cdot \exp\left(-\frac{b_i}{\varepsilon} (3 + \varepsilon)\right)}_{=: g_\varepsilon(x, y, z)} \right\|_\infty \leq \tau \quad (8)$$

for every $x, y, z \in [-1, 1]$ when

$$r \geq \frac{-\log\left(8\left(1 + \frac{6}{\varepsilon}\right)\right) \log\left(\frac{\tau}{16}\right)}{\pi^2} = \mathcal{O}(|\log(\varepsilon)|).$$

The approximation g_ε in (8) has multilinear rank (r, r, r) . In turn, the tensor $\hat{\mathcal{T}}_{ijk} = g_\varepsilon(x_i^{(1)}, x_j^{(2)}, x_k^{(3)})$ has multilinear rank at most (r, r, r) and satisfies $\|\mathcal{T} - \hat{\mathcal{T}}\|_\infty \leq \tau$.

Comparison

In Figure 1, we estimate the maximal polynomial degree required to compute a Chebyshev interpolant with accuracy $\tau = 10^{-10}$ for selected fibers of f_ε , which is a lower bound for the required polynomial degrees n_α . It perfectly matches the asymptotic behavior of the derived upper bound $\mathcal{O}(1/\log(1 + \sqrt{\varepsilon}))$. In Figure 1, we also plot the multilinear ranks from the truncated Higher Order Singular Value Decomposition (HOSVD) [15] with tolerance τ applied to the tensor containing the evaluation of f_ε on a $150 \times 150 \times 150$ Chebyshev grid. This estimate serves as a lower bound for the multilinear rank required to approximate f_ε . Due to the limited grid size, this estimate does not fully match the asymptotic behavior $|\log(\varepsilon)|$, but nonetheless it clearly reflects that the multilinear ranks can be much smaller than the polynomial degrees, as predicted by $|\log(\varepsilon)| \ll 1/\log(1 + \sqrt{\varepsilon})$, for sufficiently small ε .

3 Existing Algorithm: Chebfun3

In this section, we recall how an approximation of the form (4) is computed in Chebfun3 [29]. As discussed in Section 2.5, there are often situations in which the multilinear rank of \hat{f} is much smaller than the polynomial

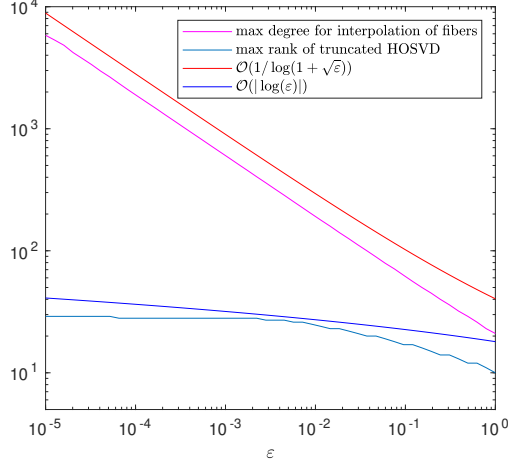


Figure 1: Theoretical upper bounds $\mathcal{O}(|\log(\varepsilon)|)$ for the multilinear rank and $\mathcal{O}(1/\log(1 + \sqrt{\varepsilon}))$ for the polynomial degree for varying ε . The maximal polynomial degree, which is used by Chebfun to approximate selected functions fibers of f_ε up to accuracy 10^{-10} . The maximal multilinear rank of the truncated HOSVD with tolerance 10^{-10} of a sample tensor on a $150 \times 150 \times 150$ Chebyshev grid. The constants in the bounds are chosen to result in curves close to the data.

degree. Chebfun3 benefits from such a situation by first using a coarse sample tensor \mathcal{T}_c to identify the fibers needed for the low-rank approximation. This allows to construct the actual approximation from a finer sample tensor \mathcal{T}_f by only evaluating these fibers instead of the whole tensor.

Chebfun 3 consists of three phases: preparation of the approximation by identifying fibers for a so called block term decomposition [14] of \mathcal{T}_c , refinement of the fibers, conversion and compression of the refined block term decomposition into Tucker format (5).

3.1 Phase 1: Block Term Decomposition

In Chebfun3, $\mathcal{T}_c \in \mathbb{R}^{n_1^{(c)} \times n_2^{(c)} \times n_3^{(c)}}$ is initially obtained by sampling f on a $17 \times 17 \times 17$ grid of Chebyshev points. A block term decomposition of \mathcal{T}_c is obtained by applying ACA [4] (see Algorithm 1) recursively. In the first step, ACA is applied to a matricization of \mathcal{T}_c , say, the mode-1 matricization $\mathcal{T}_c^{\{1\}}$. This results in index sets I, J such that

$$\mathcal{T}_c^{\{1\}} \approx \mathcal{T}_c^{\{1\}}(:, J) \left(\mathcal{T}_c^{\{1\}}(I, J) \right)^{-1} \mathcal{T}_c^{\{1\}}(I, :), \quad (9)$$

where $\mathcal{T}_c^{\{1\}}(:, J)$ contains mode-1 fibers of \mathcal{T}_c and $\mathcal{T}_c^{\{1\}}(I, :)$ contains mode-(2,3) slices of \mathcal{T}_c . For each $i \in I$, such a slice $\mathcal{T}_c^{\{1\}}(i, :)$ is reshaped into a matrix $S_i = \mathcal{T}_c(i, :, :) \in \mathbb{R}^{n_2^{(c)} \times n_3^{(c)}}$ and, in the second step, approximated by again applying ACA:

$$S_i \approx S_i(:, L_i) (S_i(K_i, L_i))^{-1} S_i(K_i, :), \quad (10)$$

where $S_i(:, L_i)$ and $S_i(K_i, :)$ contain mode-2 and mode-3 fibers of \mathcal{T}_c , respectively. Combining (9) and (10) yields the approximation

$$\mathcal{T}_c^{\{1\}} \approx \mathcal{T}_c^{\{1\}}(:, J) \left(\mathcal{T}_c^{\{1\}}(I, J) \right)^{-1} \begin{pmatrix} \text{vec}(S_1(:, L_1) (S_1(K_1, L_1))^{-1} S_1(K_1, :)) \\ \text{vec}(S_2(:, L_2) (S_2(K_2, L_2))^{-1} S_2(K_2, :)) \\ \vdots \end{pmatrix}, \quad (11)$$

where vec denotes vectorization. Reshaping this approximation into a tensor can be viewed as a block term decomposition in the sense of [14, Definition 2.2].

If the ratios of $|I|/n_1^{(c)}$, $|K_i|/n_2^{(c)}$ and $|L_i|/n_3^{(c)}$ are larger than the heuristic threshold $(2\sqrt{2})^{-1}$ the coarse grid resolution $(n_1^{(c)}, n_2^{(c)}, n_3^{(c)})$ is deemed insufficient to identify fibers. If this is the case, $n_\alpha^{(c)}$ is increased to $\lfloor \sqrt{2}^{\lceil 2 \log_2(n_\alpha^{(c)}) + 1 \rceil} \rfloor + 1$ and Phase 1 is repeated.

Algorithm 1 ACA

- 1: **Input:** matrix M , tolerance ε
 - 2: $I = []$, $J = []$
 - 3: **while** $\max |M| \geq \varepsilon$
 - 4: $(i, j) = \underset{(i,j)}{\operatorname{argmax}} |M(i, j)|$
 - 5: $I = [I, i]$, $J = [J, j]$
 - 6: $M = M - M(:, j)M(i, :)/M(i, j)$
 - 7: **Output:** index sets I and J s.t. $M \approx M(:, J)M(I, J)^{-1}M(I, :)$
-

3.2 Phase 2: Refinement

The block term decomposition (11) is composed of fibers of \mathcal{T}_c . Such a fiber $\mathcal{T}_c(:, j, k)$ corresponds to the evaluation of a univariate function $f(\cdot, y, z)$ for certain fixed y, z . Chebfun contains a heuristic to decide whether the function values in $\mathcal{T}_c(:, j, k)$ suffice to yield an accurate interpolation of $f(\cdot, y, z)$ [2]. If this is not the case, the grid is refined.

In Chebfun3 this heuristic is applied to all fibers contained in (11) in order to determine the size $n_1^{(f)} \times n_2^{(f)} \times n_3^{(f)}$, initially set to $n_1^{(c)} \times n_2^{(c)} \times n_3^{(c)}$, of the finer sample tensor \mathcal{T}_c . For each $\alpha \in \{1, 2, 3\}$, the size n_α is repeatedly increased by setting $n_\alpha^{(f)} := 2n_\alpha^{(f)} - 1$, which leads to nested Chebyshev points, until the heuristic considers the resolution sufficient for all mode- α fibers. Replacing all fibers in (11) by their refined counterparts yields an approximation of the tensor \mathcal{T}_f , which contains evaluations of f on a $n_1^{(f)} \times n_2^{(f)} \times n_3^{(f)}$ Chebyshev grid. Note that \mathcal{T}_f might be very large and is never computed explicitly.

3.3 Phase 3: Compression

In the third phase of the Chebfun3 constructor, the refined block term decomposition is converted and compressed to the desired Tucker format (5), where the interpolants $u_i(x)$ are stored as Chebfun objects [3]; see [29] for details. Lemma 1 guarantees a good approximation when the polynomial degrees $n_1^{(f)}, n_2^{(f)}, n_3^{(f)}$ are sufficiently large and when \mathcal{T}_f is well approximated by the Tucker approximation $\hat{\mathcal{T}}_f$. Neither of these properties can be guaranteed in Phases 1 and 2 alone. Therefore in a final step, Chebfun3 verifies the accuracy by comparing f and the approximation \hat{f} at Halton points [37]. If the estimated error is too large, the whole algorithm is restarted on a finer coarse grid from Phase 1.

3.4 Disadvantages

The Chebfun3 algorithm often requires unnecessarily many function evaluations. As we will illustrate in the following, this is due to redundancy among the mode-2 and mode-3 fibers. For this purpose we collect all (refined) mode-2 fibers $S_i(:, L_i)$ in the block term decomposition (11) into the columns of a big matrix $V_m^{\text{BTD}} = [S_1(:, L_1) \ \cdots \ S_m(:, L_m)]$, where m is the number of steps of the outer ACA (9). As will be demonstrated with an example below, matrix V_m^{BTD} is often observed to have low numerical rank, which in turn allows to represent its column space by much fewer columns, that is, much fewer mode-2 fibers. As the accuracy of the column space determines the accuracy of the Tucker decomposition after the compression, this implies that the other mode-2 fibers in V_m^{BTD} are redundant.

Let us now consider the block term decomposition¹ (11) for the function

$$f(x, y, z) = \frac{1}{1 + 25\sqrt{x^2 + y^2 + z^2}}.$$

In Figure 2 the numerical rank and the number of columns of V_m^{BTD} are compared. For $m = 10$ the approximation of the slices S_{i_1} to $S_{i_{10}}$ leads to a total of 153 mode-2 fibers, the sum of the corresponding red and blue bars in Figure 2. In contrast, their numerical rank (blue bar) is only 19. Thus, the red bar can be interpreted as number of redundant mode-2 fibers. This happens since nearby slices tend to be similar. The total block term decomposition contains 18 slices and is compressed into a Tucker decomposition

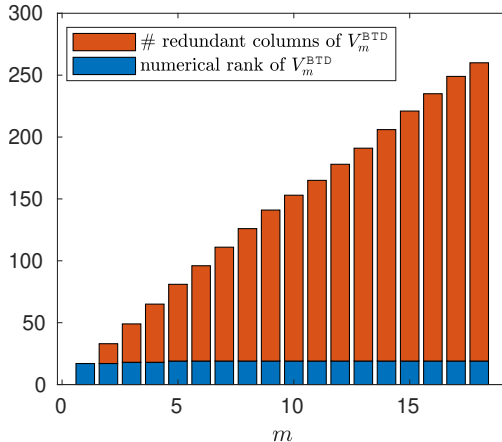


Figure 2: Numerical rank and number of redundant columns (= total number of columns - numerical rank) of the matrix V_m^{BTD} , whose columns are given by the refined version of the mode-2 fibers determined after m steps of the outer ACA (9) in Chebfun3.

with multilinear rank (17, 19, 19). It contains 242 redundant fibers, the refinement requires 192 function evaluations for each of them. Note that the asymmetry in the rank of the Tucker decomposition is caused by the asymmetry of the block term decomposition.

Another disadvantage is that Chebfun3 always requires the full evaluation of \mathcal{T}_c in Phase 1. This becomes expensive when a large size $n_1^{(c)} \times n_2^{(c)} \times n_3^{(c)}$ is needed in order to properly identify suitable fibers.

4 Novel Algorithm: Chebfun3F

In this section, we describe our novel algorithm Chebfun3F to compute an approximation of the form (5). The goal of Chebfun3F is to avoid the redundant function evaluations observed in Chebfun3. While the structure of Chebfun3F is similar to Chebfun3, consisting of 3 phases to identify/refine fibers and compute a Tucker decomposition, there is a major difference in Phase 1. Instead of proceeding via slices, we directly identify mode- α fibers of \mathcal{T}_c for building factor matrices. The core tensor is constructed in Phase 3.

4.1 Phase 1: Fiber Indices and Factor Matrices

As in Chebfun3, the coarse tensor $\mathcal{T}_c \in \mathbb{R}^{n_1^{(c)} \times n_2^{(c)} \times n_3^{(c)}}$ is initially defined to contain the function values of f on a $17 \times 17 \times 17$ Chebyshev grid. We seek to compute factor matrices $U_c \in \mathbb{R}^{n_1^{(c)} \times r_1}$, $V_c \in \mathbb{R}^{n_2^{(c)} \times r_2}$ and

¹Note that the accuracy verification in Phase 3 fails once for this function. Here we only consider to block term decomposition obtained after restarting the procedure.

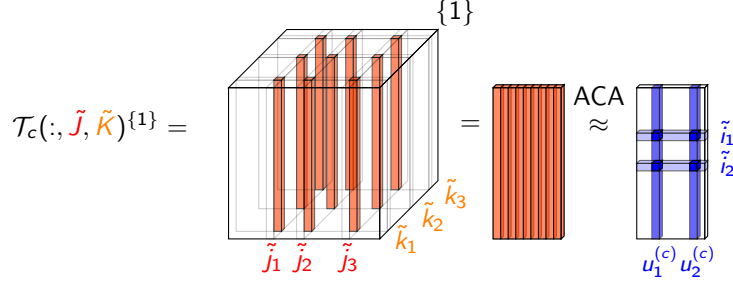


Figure 3: Visualization of applying ACA (Algorithm 1) to a matricization of a subtensor.

$W_c \in \mathbb{R}^{n_3^{(c)} \times r_3}$ such that the orthogonal projection of \mathcal{T}_c onto the span of the factor matrices is an accurate approximation of T_c , i.e.

$$\mathcal{T}_c \approx \mathcal{T}_c \times_1 U_c (U_c^T U_c)^{-1} U_c^T \times_2 V_c (V_c^T V_c)^{-1} V_c^T \times_3 W_c (W_c^T W_c)^{-1} W_c^T. \quad (12)$$

Additionally, we require that the columns in U_c, V_c, W_c contain fibers of \mathcal{T}_c .

In the existing literature, algorithms to compute such factor matrices include the Higher Order Interpolatory Decomposition [46], which is based on a rank revealing QR decomposition, and the Fiber Sampling Tensor Decomposition [9], which is a generalization of the CUR decomposition. We propose a novel algorithm, which in contrast to the existing algorithms does not require the evaluation of the full tensor \mathcal{T}_c . We follow the ideas of TT-cross [40, 48] and its variants such as the Schur-Cross3D [45] and the ALS-cross [18].

Initially, we randomly choose index sets $\tilde{I}, \tilde{J}, \tilde{K}$ each containing 6 indices. In the first step, we apply Algorithm 1 to $(\mathcal{T}_c(:, \tilde{J}, \tilde{K}))^{\{1\}}$. Note that this needs drawing only $36 \cdot n_1^{(c)}$ values of the function f , in contrast to $n_1^{(c)} n_2^{(c)} n_3^{(c)}$ values in the whole tensor \mathcal{T}_c . The selected r_1 columns serve as a first candidate for the factor matrix U_c . The index set \tilde{I} is set to the row indices selected by Algorithm 1 (see Figure 3). We use the updated index set and apply Algorithm 1 to $(\mathcal{T}_c(\tilde{I}, : \tilde{K}))^{\{1\}}$ analogously, which yields V_c and an updated \tilde{J} . From $(\mathcal{T}_c(\tilde{I}, \tilde{J}, :))^{\{1\}}$ we obtain W_c and \tilde{J} . We repeat this process in an alternating fashion with the updated index sets, which leads to potentially improved factor matrices. Following the ideas of Chebfun3, we check after each iteration whether the ratios $r_1/n_1^{(c)}$, $r_2/n_2^{(c)}$ and $r_3/n_3^{(c)}$ surpass the heuristic threshold $(2\sqrt{2})^{-1}$. If this is the case, we increase the size of the coarse tensor $n_\alpha^{(c)}$ to $\lfloor \sqrt{2}^{\lfloor 2 \log_2(n_\alpha^{(c)}) + 1 \rfloor} \rfloor + 1$ and restart the whole process by reinitializing $\tilde{I}, \tilde{J}, \tilde{K}$ with r_1, r_2, r_3 random indices respectively.

It is not clear a priori how many iterations are needed to attain an approximation (12) that yields a Tucker approximation (5) which passes the accuracy verification in Phase 3. In numerical experiments, it has usually proven to be sufficient to stop after the second iteration, during which the coarse grid has not been refined, or when $|\tilde{I}| \leq 1$, $|\tilde{J}| \leq 1$ or $|\tilde{K}| \leq 1$. This is formalized in Algorithm 2. In many cases, we found that the numbers of columns in the factor matrices are equal to the multilinear rank of the truncated HOSVD [15] of \mathcal{T}_c with the same tolerance.

4.2 Phase 2: Refinement of the Factors

In Phase 2, the fibers in U_c, V_c, W_c are refined using Chebfun's heuristic [2] as in Chebfun3 (see Section 3.2). This leads to new factor matrices $U_f \in \mathbb{R}^{n_1^{(f)} \times r_1}$, $V_f \in \mathbb{R}^{n_2^{(f)} \times r_2}$ and $W_f \in \mathbb{R}^{n_3^{(f)} \times r_3}$ containing the refined fibers of \mathcal{T}_f , corresponding to the evaluations of f on a $n_1^{(f)} \times n_2^{(f)} \times n_3^{(f)}$ Chebyshev grid. This phase needs only $\mathcal{O}(\sum_\alpha n_\alpha^{(f)} r_\alpha)$ evaluations of f .

4.3 Phase 3: Reconstruction of the Core Tensor

In the final Phase of Chebfun3F, we compute a core tensor $\hat{\mathcal{C}}$ to yield an approximation $\mathcal{T}_f \approx \hat{\mathcal{C}} \times_1 U_f \times_2 V_f \times_3 W_f$.

Algorithm 2 Factor Matrix Computation

- 1: **Input:** $f, (n_1^{(c)}, n_2^{(c)}, n_3^{(c)}), (r_1, r_2, r_3)$
 - 2: Let $T_c(i, j, k) = f(x_i^{(1)}, x_j^{(2)}, x_k^{(3)})$ be a function that evaluates the values of f on a $n_1^{(c)} \times n_2^{(c)} \times n_3^{(c)}$ Chebyshev grid on demand.
 - 3: initialize \tilde{J}, \tilde{K} with r_2, r_3 randomly chosen indices in $\{1, \dots, n_1^{(c)}\}, \{1, \dots, n_2^{(c)}\}$
 - 4: **for** iterations = 1:2
 - 5: compute ACA of $\mathcal{T}_c(:, \tilde{J}, \tilde{K})^{\{1\}} \rightarrow U_c \in \mathbb{R}^{n_1^{(c)} \times r_1} =$ selected columns, $\tilde{I} =$ selected row indices
 - 6: compute ACA of $\mathcal{T}_c(\tilde{I}, :, \tilde{K})^{\{2\}} \rightarrow V_c \in \mathbb{R}^{n_2^{(c)} \times r_2} =$ selected columns, $\tilde{J} =$ selected row indices
 - 7: compute ACA of $\mathcal{T}_c(\tilde{I}, \tilde{J}, :)^{\{3\}} \rightarrow W_c \in \mathbb{R}^{n_3^{(c)} \times r_3} =$ selected columns, $\tilde{K} =$ selected row indices
 - 8: **if** the multilinear ranks get too large \rightarrow adjust the size of $(n_1^{(c)}, n_2^{(c)}, n_3^{(c)})$ and go to line 2
 - 9: **if** $r_1 \leq 1$ or $r_2 \leq 1$ or $r_3 \leq 1 \rightarrow$ go to line 10
 - 10: **Output:** $U_c, V_c, W_c, (n_1^{(c)}, n_2^{(c)}, n_3^{(c)}), (r_1, r_2, r_3)$
-

In principle, the best approximation (with respect to the Frobenius norm) for fixed factor matrices U_f, V_f, W_f is obtained by orthogonal projections [15]. Such an approach comes with the major disadvantage that the full evaluation of \mathcal{T}_f is required. This can be circumvented by instead using oblique projections $U_f(\Phi_I^T U_f)^{-1} \Phi_I^T$, where $\Phi_I^T U = U(I, :)$ for an index set $I \subset \{1, \dots, n_1^{(f)}\}$. Oblique projections in all three modes yield

$$\mathcal{T}_f \approx \hat{\mathcal{T}} = \underbrace{(\mathcal{T}_f(I, J, K) \times_1 (\Phi_I^T U_f)^{-1} \times_2 (\Phi_J^T V_f)^{-1} \times_3 (\Phi_K^T W_f)^{-1})}_{=\hat{\mathcal{C}}} \times_1 U_f \times_2 V_f \times_3 W_f,$$

for index sets I, J, K . The choice of I, J, K is crucial for the approximation quality and will be discussed later on. The computation of the core tensor $\hat{\mathcal{C}}$ only requires $r_1 r_2 r_3$ evaluations in Phase 3. From $\hat{\mathcal{T}}$ we construct the approximation (5) as described in Section 2.3.

In practice, instead of using the potentially ill-conditioned matrices $(\Phi_I^T U_f)^{-1}, (\Phi_J^T V_f)^{-1}, (\Phi_K^T W_f)^{-1}$ we compute QR decompositions $U_f = Q_U R_U, V_f = Q_V R_V, W_f = Q_W R_W$, and use the equivalent representation

$$\hat{\mathcal{T}} = \mathcal{T}_f(I, J, K) \times_1 Q_U (\Phi_I^T Q_U)^{-1} \times_2 Q_V (\Phi_J^T Q_V)^{-1} \times_3 Q_W (\Phi_K^T Q_W)^{-1}$$

in Chebfun3F. The evaluation of $\mathcal{T}_f(I, J, K)$ requires $r_1 r_2 r_3$ samples from f .

The following lemma plays a critical role in guiding the choice of indices I, J, K .

Lemma 2 ([11, Lemma 7.3]). *Let $M \in \mathbb{R}^{n \times m}$, $n \geq m$, have orthonormal columns. Consider an index set $I \subset \{1, \dots, n\}$ of cardinality m such that $\Phi_I^T M$ is invertible. Then the oblique projection $M(\Phi_I^T M)^{-1} \Phi_I^T$ satisfies*

$$\|x - M(\Phi_I^T M)^{-1} \Phi_I^T x\|_2 \leq \|(\Phi_I^T M)^{-1}\|_2 \cdot \|(I - MM^T)x\|_2, \quad \forall x \in \mathbb{R}^n,$$

where $\|\cdot\|_2$ denotes the matrix 2-norm.

Lemma 2 exhibits the critical role played by the quantity $\|(\Phi_I^T Q_U)^{-1}\|_2 \geq 1$ for oblique projections. In Chebfun3, we use the *discrete empirical interpolation method* (DEIM) [10], presented in Algorithm 3, to compute the index sets I, J, K given Q_U, Q_V, Q_W . In practice, these index sets usually yield good approximations as $\|(\Phi_I^T Q_U)^{-1}\|_2$ tends to be small; see also Section 4.4.1.

4.4 Chebfun3F Algorithm

Given the tensor approximation $\hat{\mathcal{T}}$, we obtain \hat{f} by interpolating the factor matrices as described in Section 2.3. Using Chebfun [3], the columns in U_f, V_f, W_f are transformed into Chebyshev interpolants. Following Chebfun3, we perform an accuracy verification for \hat{f} by comparing its evaluations at Halton points to

Algorithm 3 Discrete Empirical Interpolation Method

- 1: **Input:** orthonormal matrix $M \in \mathbb{R}^{n \times m}$
 - 2: $I = [\operatorname{argmax} |M(:, 1)|]$
 - 3: **for** $k = 2, \dots, m$
 - 4: $c = M(I, 1 : k - 1) \setminus M(I, k)$
 - 5: $r = M(:, k) - M(:, 1 : k - 1)c$
 - 6: $I = [I, \operatorname{argmax} |r|]$
 - 7: **Output:** index set I
-

the original f . If the difference of the evaluations is too large, we restart the whole algorithm using a finer coarse grid. Additionally, we modify the ranks such that if $r_{\alpha_1} \leq 2$ we set $r_{\alpha_2} = \max(6, 2r_{\alpha_2})$ and $r_{\alpha_1} = 3$ for $\alpha_1 \neq \alpha_2$. This ensures that the multilinear ranks can grow in Phase 1. The overall Chebfun3F algorithm is formalized in Algorithm 4.

Algorithm 4 Chebfun3F

- 1: **Input:** f
 - 2: **Initialization:** $(n_1^{(c)}, n_c^{(c)}, n_3^{(c)}) = (17, 17, 17)$, $(r_1, r_2, r_3) = (6, 6, 6)$
 - 3: **Phase 1:**
 - 4: apply Algorithm 2 to compute the factor matrices U_c, V_c, W_c and to update $(n_1^{(c)}, n_2^{(c)}, n_3^{(c)})$, (r_1, r_2, r_3)
 - 5: **Phase 2:**
 - 6: $(n_1^{(f)}, n_2^{(f)}, n_3^{(f)}) = (n_1^{(c)}, n_2^{(c)}, n_3^{(c)})$, $U_f = U_c, V_f = V_c, W_f = W_c$
 - 7: **while** Chebfun heuristic in [2] to decide if U_f contains a sufficient number of entries is not satisfied
 - 8: $n_1^{(f)} = 2n_1^{(f)} - 1$, refine U_f such that its columns have length $n_1^{(f)}$
 - 9: proceed analogously to obtain V_f, W_f
 - 10: **Phase 3:**
 - 11: $[Q_U, R_U] = \operatorname{qr}(U_f)$, $I = \operatorname{DEIM}(Q_U)$, $U = Q_U \cdot Q_U(I, :)^{-1}$
 - 12: $[Q_V, R_V] = \operatorname{qr}(V_f)$, $J = \operatorname{DEIM}(Q_V)$, $V = Q_V \cdot Q_V(J, :)^{-1}$
 - 13: $[Q_W, R_W] = \operatorname{qr}(W_f)$, $K = \operatorname{DEIM}(Q_W)$, $W = Q_W \cdot Q_W(K, :)^{-1}$
 - 14: compute the Chebyshev interpolants $U(x), V(y), W(z)$ (see Section 2.3)
 - 15: $\mathcal{C} = T_f(I, J, K)$, $\hat{f}(x, y, z) \approx \mathcal{C} \times_1 U(x) \times_2 V(y) \times_3 W(z)$
 - 16: **if** $|f(x, y, z) - \hat{f}(x, y, z)| > 10\varepsilon$ at Halton points $(x, y, z) \in [-1, 1]^3$
 - 17: modify the ranks r_α if they are too small
 - 18: restart from Phase 1 with $n_\alpha^{(c)} = \lfloor \sqrt{2} \lceil 2^{\log_2(n_\alpha^{(c)})+1} \rceil \rfloor + 1$
 - 19: **Output:** approximation $\hat{f}(x, y, z) = \mathcal{C} \times_1 U(x) \times_2 V(y) \times_3 W(z)$
-

Remark. In Chebfun3 upper bounds for the multilinear rank, polynomial degree and grid sizes are prescribed. The tolerances in the accuracy verification and in the ACA are initially set close to machine precision or provided by the user. Tolerance issues are avoided by relaxing these tolerances adaptively based on the computed function evaluations. In Chebfun3F, we handle these technicalities in the same manner.

4.4.1 Existence of a Quasi-Optimal Chebfun3F Approximation

Due to the many heuristic ingredients in the Chebfun3F algorithm, it is difficult to analyze the convergence of the whole algorithm. Instead, we discuss the existence and error analysis of a specific Chebfun3F reconstruction. Lemma 1 shows how we can bound the approximation error depending on $\|\mathcal{T} - \hat{\mathcal{T}}\|_\infty$. Theorem 2 below provides a bound for this error for \hat{T} for specifically chosen fibers and index sets. The best approximation in the format will be at least as good. Although Chebfun3F is not guaranteed to return the best approximation, it is hoped that its error is not too far away.

Theorem 2. Consider $\mathcal{T} \in \mathbb{R}^{n_1 \times n_2 \times n_3}$ of multilinear rank at least (r_1, r_2, r_3) . Let Q_U, Q_V, Q_W denote orthonormal bases of r_1, r_2, r_3 selected mode-1, 2, 3 fibers of \mathcal{T} respectively. Given index sets I, J, K we consider a Tucker decomposition of the form

$$\hat{\mathcal{T}} = \mathcal{T} \times_1 Q_U (\Phi_I^T Q_U)^{-1} \Phi_I^T \times_2 Q_V (\Phi_J^T Q_V)^{-1} \Phi_J^T \times_3 Q_W (\Phi_K^T Q_W)^{-1} \Phi_K^T,$$

where $\Phi_I^T U = U(I, :)$. There exists a choice of fibers and indices such that

$$\begin{aligned} \|\mathcal{T} - \hat{\mathcal{T}}\|_\infty \leq & \left(\sqrt{(1+r_1(n_1-1))(r_1+1)} + \sqrt{(1+r_1(n_1-1))(1+r_2(n_2-1))(r_2+1)} \right. \\ & \left. + \sqrt{(1+r_1(n_1-1))(1+r_2(n_2-1))(1+r_3(n_3-1))(r_3+1)} \right) \|\mathcal{T} - \hat{\mathcal{T}}_{\text{best}}\|_F, \end{aligned}$$

where $\|\cdot\|_F$ denotes the Frobenius norm and $\hat{\mathcal{T}}_{\text{best}}$ is the best Tucker approximation of \mathcal{T} with multilinear rank at most (r_1, r_2, r_3) .

Proof. Using Frobenius norm properties and Lemma 2, we obtain

$$\begin{aligned} \|\mathcal{T} - \hat{\mathcal{T}}\|_\infty \leq & \|\mathcal{T} - \hat{\mathcal{T}}\|_F \leq \|(\Phi_I^T Q_U)^{-1}\|_2 \|(I - Q_U Q_U^T) \mathcal{T}^{\{1\}}\|_F \\ & + \|(\Phi_I^T Q_U)^{-1}\|_2 \|(\Phi_J^T Q_V)^{-1}\|_2 \|(I - Q_V Q_V^T) \mathcal{T}^{\{2\}}\|_F \\ & + \|(\Phi_I^T Q_U)^{-1}\|_2 \|(\Phi_J^T Q_V)^{-1}\|_2 \|(\Phi_K^T Q_W)^{-1}\|_2 \|(I - Q_W Q_W^T) \mathcal{T}^{\{3\}}\|_F. \end{aligned} \quad (13)$$

From [21, Lemma 2.1] it follows that there exists an index set I such that

$$\|(\Phi_I^T U)^{-1}\|_2 \leq \sqrt{1+r_1(n_1-r_1)}. \quad (14)$$

From [17, Theorem 8] it follows that we can select mode-1 fibers of \mathcal{T} such that

$$\|(I - Q_U Q_U^T) \mathcal{T}^{\{1\}}\|_F = \|(I - U(U^T U)^{-1} U^T) \mathcal{T}^{\{1\}}\|_F \leq \sqrt{r_1+1} \|\mathcal{T} - \hat{\mathcal{T}}_{\text{best}}\|_F. \quad (15)$$

Analogous bounds hold for $\|(\Phi_J^T Q_V)^{-1}\|_2$, $\|(\Phi_K^T Q_W)^{-1}\|_2$, $\|(I - Q_V Q_V^T) \mathcal{T}^{\{2\}}\|_F$ and $\|(I - Q_W Q_W^T) \mathcal{T}^{\{3\}}\|_F$. Applying the bounds (14) and (15) to the factors in (13) yields the claimed result. \square

Remark. If one uses orthogonal instead of oblique projections in Phase 3, Corollary 6 in [13] yields a bound similar to Theorem 2.

4.4.2 Comparison of Theoretical Cost

Assume f can be approximated accurately in Tucker format (5) with multilinear rank (r, r, r) and polynomial degrees (n, n, n) , $n \geq r$. In a highly idealized setting Chebfun3 and Chebfun3F refine the coarse grid in Phase 1 until $n_\alpha^{(c)} > (2\sqrt{2})r$ and identify fibers on this coarse grid. These fibers are refined until $n_\alpha^{(f)} \geq n$ and lead to Tucker approximations which pass the accuracy check in Phase 3. Under these circumstances, both Chebfun3 and Chebfun3F use $\mathcal{O}(r^3)$ function evaluations in Phase 1 (see Section 2.2 in [29]). In total, Chebfun3 requires $\mathcal{O}(nr^2)$ function evaluations [29, Proposition 2.1]), whereas Chebfun3F only requires $\mathcal{O}(r^3 + nr)$, since fewer fibers are refined in Phase 2. We want to emphasize that, in general, it is not guaranteed that this $n_\alpha^{(c)}$ suffices to identify fibers leading to an accurate approximation.

5 Numerical Results

In this section, we present numerical experiments to compare Chebfun3F and Chebfun3.² The main focus lies on the number of function evaluations required to compute the approximation in Tucker format (5). Unless mentioned otherwise the tolerance for the ACA and the accuracy check are initially set close to machine precision.

²The Matlab code to reproduce these results is available from <https://github.com/cstroessner/Chebfun3F>.

5.1 Chebfun3 vs. Chebfun3F

In Section 3.4 we illustrated that the function

$$f(x, y, z) = \frac{1}{1 + 25\sqrt{x^2 + y^2 + z^2}},$$

leads to a lot of redundant fibers in Chebfun3. For this function, for both Chebfun3 and Chebfun3F, the accuracy check at the end of Phase 3 fails and the computation is restarted on a finer coarse grid, which leads to an approximation that passes the test. Overall 903 364 function evaluations are required by Chebfun3, 421 041 of them are used before the restart. In comparison, Chebfun3F only needs 222 546 function evaluation in total and 100 496 before the restart. In the final accuracy check, the estimated error for Chebfun3 is $7.8 \cdot 10^{-13}$ and $3.6 \cdot 10^{-13}$ for Chebfun3F, i.e. both approximations achieve around the same accuracy.

In Figure 4, the function evaluations per phase are juxtaposed. The figure shows, that Chebfun3 requires a large number of function evaluations in Phase 2. This is caused by the redundant fibers. In Phase 1, Chebfun3F requires fewer function evaluations, since \mathcal{T}_c is not evaluated completely. Whilst Chebfun3 only requires function evaluations in Phase 3 for the accuracy check, Chebfun3F additionally needs to compute the core tensor, which only leads to a small number of function evaluations compared to the other phases.

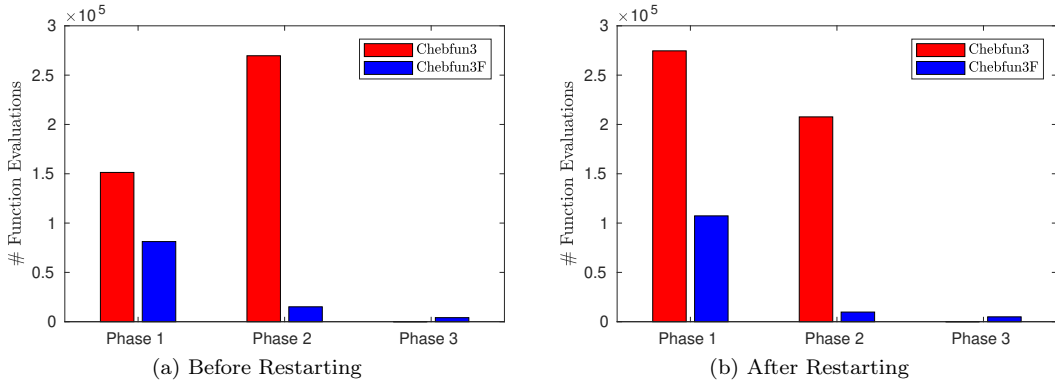


Figure 4: Comparison of the function evaluations used by Chebfun3 and Chebfun3F to approximate $f(x, y, z) = (1 + 25\sqrt{x^2 + y^2 + z^2})^{-1}$. Both algorithms are restarted due to failing the accuracy check once. Evaluations in the before the restart are depicted in (a), evaluations after the restart in (b). The evaluations are subdivided into phases corresponding to the phases in Section 3 and Section 4 respectively.

In Figure 5, the required function evaluations are depicted for four different functions. Again both algorithms lead to approximations of similar accuracy and Chebfun3F requires fewer function evaluations than Chebfun3. For

$$f_1(x, y, z) = \exp(-\sqrt{(x-1)^2 + (y-1)^2 + (z-1)^2}) \quad (16)$$

Chebfun3 requires the refinement of a huge number of redundant fibers in Phase 2. The evaluations for

$$f_2(x, y, z) = \cosh 3(x + y + z)^{-2} \quad (17)$$

differ most in Phase 1, where Chebfun3F benefits from not evaluating \mathcal{T}_c completely. No additional refinement is required in Phase 2. For the function

$$f_3(x, y, z) = \frac{10^5}{1 + 10^5(x^2 + y^2 + z^2)}. \quad (18)$$

Chebfun3F reduces the number of required function evaluations by more than 98% to 1 603 693 from 1 092 693 332 required by Chebfun3.

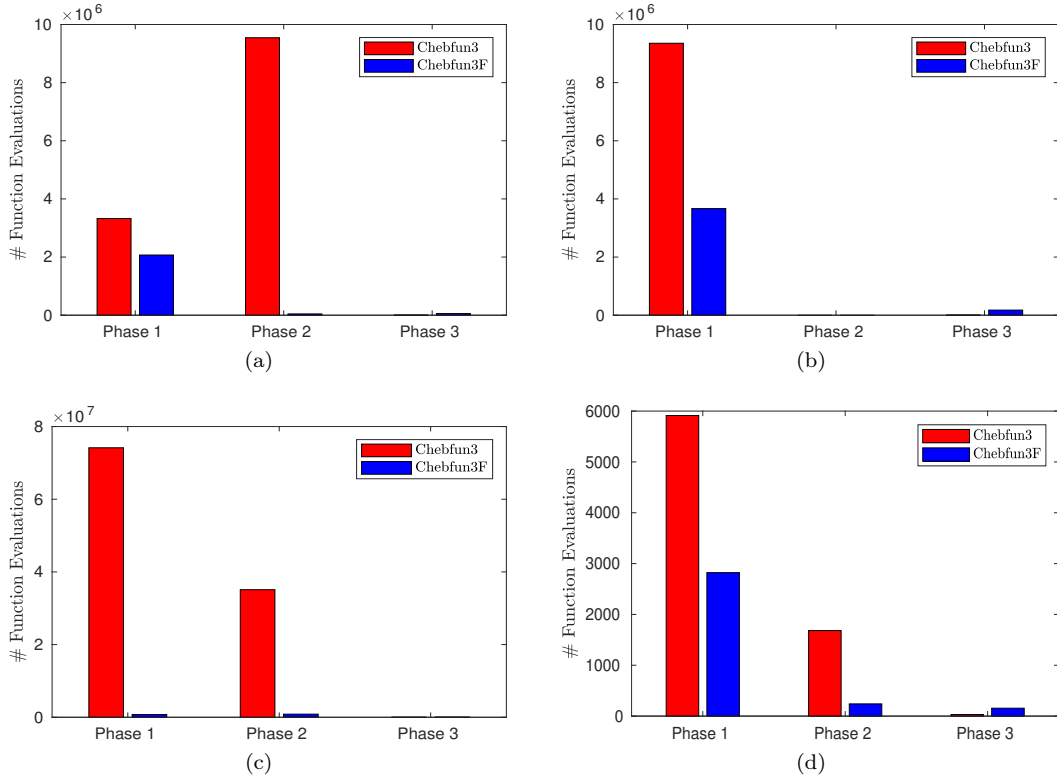


Figure 5: Total number of function evaluations per Phase in Chebfun3 and Chebfun3F for the functions: (a) f_1 (b) f_2 , (c) f_3 as defined in (16)-(18) (d) the parametric PDE model (19)-(20) with prescribed tolerance 10^{-9} .

In certain cases Chebfun3 outperforms Chebfun3F. This can happen in degenerated situations. For instance, the function $f(x, y, z) = \tanh(5(x + z)) \exp(y)$ requires an Tucker decomposition with rank $r = [71, 1, 71]$. In this case, Chebfun3F heavily relies on the heuristic to increase (r_1, r_2, r_3) when restarting and requires 1 641 712 function evaluations compared to 1 128 061 in Chebfun3. Other functions that are difficult to approximate with Chebfun3F include locally supported functions, for which identifying fibers in Phase 1 without fully evaluating \mathcal{T}_c might be difficult.

Application: Uncertainty Quantification

Algorithms in uncertainty quantification, such as the Metropolis-Hastings method, often require the repeated evaluations of a parameter depended quantity of interest [50]. In many applications, the evaluation of this quantity requires the solution of a PDE depending on the parameters. To speed up computations, the mapping from the parameters to the quantity of interest is often replaced by a surrogate model [57]. In the context of models with three parameters (or after a dimension reduction to three parameters [12]), Chebfun3/Chebfun3F could be a suitable surrogate.

We consider the parametric elliptic PDE model problem on $\Omega = [-1, 1]^2$

$$\nabla \cdot ((p_1 + 2)f_1(x, y) + (p_2 + 2)f_2(x, y) + (p_3 + 2)f_3(x, y))(\nabla u(x, y)) = 1 \quad (x, y) \in \Omega, \quad (19)$$

$$u(x, y) = 0 \quad \in \delta\Omega, \quad (20)$$

with parameters $(p_1, p_2, p_3) \in [-1, 1]^3$ and functions $f_1(x, y) = \cos(x) + \sin(y) + 2$, $f_2(x, y) = \sin(x) + \cos(y) + 2$, and $f_3(x, y) = \cos(x^2 + y^2) + 2$. The quantity of interest is defined as point evaluation $u(0.5, 0.5)$. With

Chebfun3F, we only need 3,217 PDE solves to compute an approximation with prescribed accuracy 10^{-9} , whereas Chebfun3 requires 7,626 as depicted in Figure 5(d).

5.2 Comparison to Sparse Grids

Lastly, we study how efficient Chebfun3 approximations are compared to sparse grids [8]. Sparse grids are a method to interpolate functions by projecting them onto a particular space. This space is obtained by selecting the most beneficial elements from a hierarchical basis under the assumption that the function has bounded mixed second derivatives. Interpolation based on sparse grids performs particularly well when the norms of the mixed second derivatives of the function are small. In the following, we use dimension adaptive sparse grids based on a Chebyshev-Gauss-Lobatto grid with polynomial basis functions from the Sparse Grid Interpolation Toolbox[32].

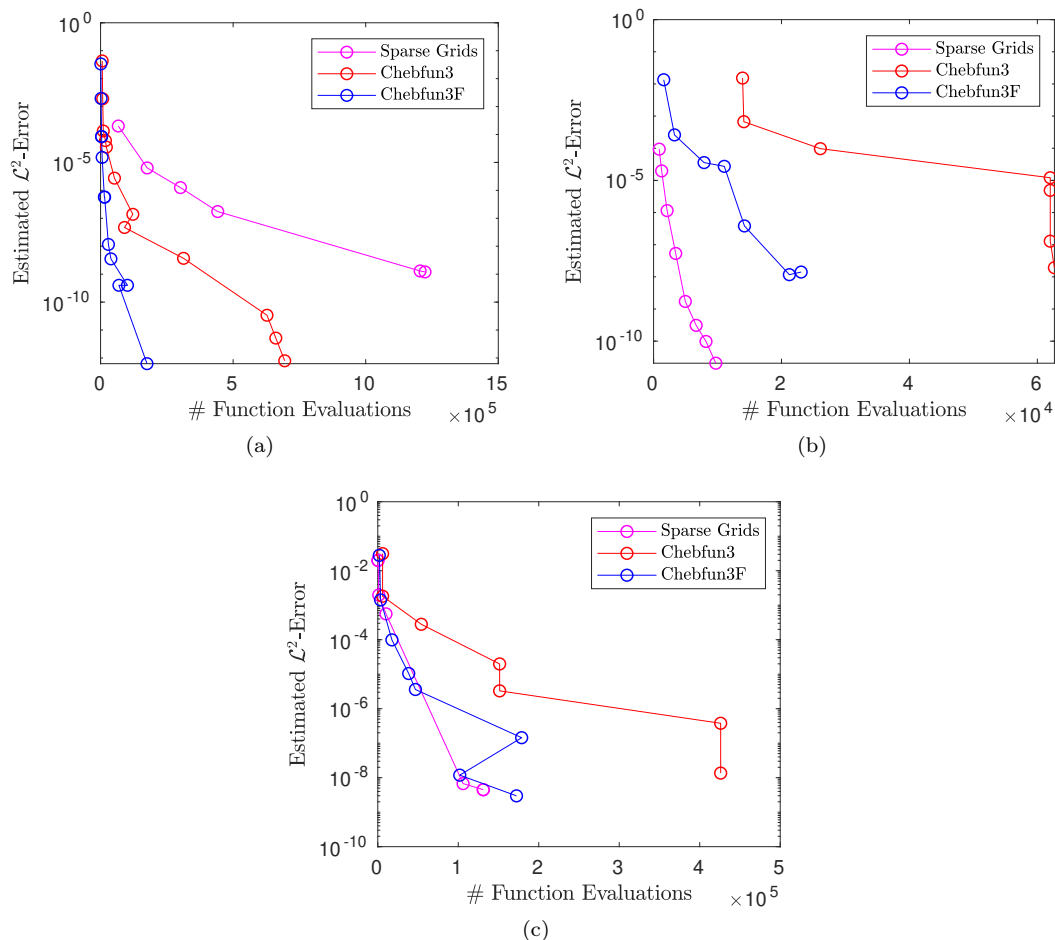


Figure 6: Comparison of the number of function evaluations required to compute a Chebfun3, Chebfun3F and sparse grid approximation for the functions: (a) $f(x, y, z) = (1 + 25\sqrt{x^2 + y^2 + z^2})^{-1}$, (b) sum of 10 Gaussians, (c) $f_4(21)$. The algorithms are initialized with varying tolerances. Their \mathcal{L}^2 error is estimated at 1000 sample points.

We compare how the approximation error decays compared to the number of function evaluations. Therefore, we prescribe varying tolerances to the algorithms. In Figure 6 the error decay is plotted for sparse grids, Chebfun3 and Chebfun3F. In (a), the function already studied in section 3.4 is depicted. We observe that

both Chebfun3F and Chebfun3 require fewer function evaluations than sparse grids to achieve the same accuracy. The sparse grids perform poorly, since the function is smooth, but the norms of the second mixed derivatives are rather large. In contrast, the sum of 10 Gaussians depicted in (b) is well suited for sparse grids. In this case sparse grids require fewer function evaluations than Chebfun3F and Chebfun3 for the same accuracy. In (c) the Chebfun3F and sparse grids perform about equally well for

$$f_4(x, y, z) = \log(x + yz + \exp(xyz) + \cos(\sin(\exp(xyz))))). \quad (21)$$

For an arbitrary, black-box function it is not clear a priori whether a sparse grid interpolation or a Tucker decomposition (5) is the more efficient type of approximation, but we can expect that if the Tucker decomposition is a better approximation format, Chebfun3F is a more efficient algorithm to take advantage of it compared to Chebfun3F.

6 Conclusions

Trivariate functions defined on tensor product domains can be approximated efficiently by combining tensorized Chebyshev interpolation and a low-rank Tucker approximation of the evaluation tensor. In this paper, we presented Chebfun3F to compute such approximations. Our numerical experiments show that Chebfun3F requires fewer function evaluations to compute such an approximation of the same accuracy compared to Chebfun3. Future work could cover how operations can be computed directly on the level of Tucker decompositions. For instance, multiplication can be treated directly on the tensor level [34], whereas the Chebfun3 package relies on constructing a new approximation from point evaluations. We suspect that other operations can be computed in a similar manner.

Finally, let us remark that the extension of the presented algorithms and results to functions depending on more than three variables is trivial. However, the Tucker format is not well suited for the high-order tensors arising from the evaluation of a function in many variables. Other formats, such as the TT format, are better suited for this purpose and will require different construction algorithms.

References

- [1] K. W. AITON AND T. A. DRISCOLL, *An adaptive partition of unity method for Chebyshev polynomial interpolation*, SIAM J. Sci. Comput., 40 (2018), pp. A251–A265.
- [2] J. L. AURENTZ AND L. N. TREFETHEN, *Chopping a Chebyshev series*, ACM Trans. Math. Software, 43 (2017), pp. Art. 33, 21.
- [3] Z. BATTLES AND L. N. TREFETHEN, *An extension of MATLAB to continuous functions and operators*, SIAM J. Sci. Comput., 25 (2004), pp. 1743–1770.
- [4] M. BEBENDORF, *Adaptive cross approximation of multivariate functions*, Constr. Approx., 34 (2011), pp. 149–179.
- [5] J.-P. BERRUT AND L. N. TREFETHEN, *Barycentric Lagrange interpolation*, SIAM Rev., 46 (2004), pp. 501–517.
- [6] D. BIGONI, A. P. ENGSIG-KARUP, AND Y. M. MARZOUK, *Spectral tensor-train decomposition*, SIAM J. Sci. Comput., 38 (2016), pp. A2405–A2439.
- [7] D. BRAESS AND W. HACKBUSCH, *Approximation of $1/x$ by exponential sums in $[1, \infty)$* , IMA J. Numer. Anal., 25 (2005), pp. 685–697.
- [8] H.-J. BUNGARTZ AND M. GRIEBEL, *Sparse grids*, Acta Numer., 13 (2004), pp. 147–269.

- [9] C. F. CAIAFA AND A. CICHOCKI, *Generalizing the column-row matrix decomposition to multi-way arrays*, *Linear Algebra Appl.*, 433 (2010), pp. 557–573.
- [10] S. CHATURANTABUT AND D. C. SORENSEN, *Discrete empirical interpolation for nonlinear model reduction*, in *Proceedings of the 48th IEEE Conference on Decision and Control and the 2009 28th Chinese Control Conference*, Dec 2009, pp. 4316–4321.
- [11] S. CHATURANTABUT AND D. C. SORENSEN, *Nonlinear model reduction via discrete empirical interpolation*, *SIAM J. Sci. Comput.*, 32 (2010), pp. 2737–2764.
- [12] P. G. CONSTANTINE, C. KENT, AND T. BUI-THANH, *Accelerating Markov chain Monte Carlo with active subspaces*, *SIAM J. Sci. Comput.*, 38 (2016), pp. A2779–A2805.
- [13] A. CORTINOVIS AND D. KRESSNER, *Low-rank approximation in the Frobenius norm by column and row subset selection*, *arXiv e-prints*, (2019), p. arXiv:1908.06059.
- [14] L. DE LATHAUWER, *Decompositions of a higher-order tensor in block terms. II. Definitions and uniqueness*, *SIAM J. Matrix Anal. Appl.*, 30 (2008), pp. 1033–1066.
- [15] L. DE LATHAUWER, B. DE MOOR, AND J. VANDEWALLE, *A multilinear singular value decomposition*, *SIAM J. Matrix Anal. Appl.*, 21 (2000), pp. 1253–1278.
- [16] A. DEKTOR AND D. VENTURI, *Dynamically orthogonal tensor methods for high-dimensional nonlinear PDEs*, *J. Comput. Phys.*, 404 (2020), pp. 109125, 31.
- [17] A. DESHPANDE AND L. RADEMACHER, *Efficient volume sampling for row/column subset selection*, in *2010 IEEE 51st Annual Symposium on Foundations of Computer Science—FOCS 2010*, IEEE Computer Soc., Los Alamitos, CA, 2010, pp. 329–338.
- [18] S. DOLGOV AND R. SCHEICHL, *A hybrid alternating least squares-TT-cross algorithm for parametric PDEs*, *SIAM/ASA J. Uncertain. Quantif.*, 7 (2019), pp. 260–291.
- [19] T. A. DRISCOLL, N. HALE, AND L. N. TREFETHEN, *Chebfun guide*, Pafnuty Publications, Oxford, 2014.
- [20] A. FALCÓ, W. HACKBUSCH, AND A. NOUY, *Tree-based tensor formats*, *SeMA Journal*, (2018).
- [21] S. A. GOREINOV, E. E. TYRTYSHNIKOV, AND N. L. ZAMARASHKIN, *A theory of pseudoskeleton approximations*, *Linear Algebra Appl.*, 261 (1997), pp. 1–21.
- [22] A. GORODETSKY, *Continuous low-rank tensor decompositions, with applications to stochastic optimal control and data assimilation*, PhD thesis, Massachusetts Institute of Technology, Cambridge, MA, 2017.
- [23] A. GORODETSKY, S. KARAMAN, AND Y. MARZOUK, *A continuous analogue of the tensor-train decomposition*, *Computer Methods in Applied Mechanics and Engineering*, 347 (2019), pp. 59 – 84.
- [24] M. GRIEBEL AND H. HARBRECHT, *Analysis of tensor approximation schemes for continuous functions*, *arXiv e-prints*, (2019), p. arXiv:1903.04234.
- [25] W. HACKBUSCH, *Tensor spaces and numerical tensor calculus*, vol. 42 of *Springer Series in Computational Mathematics*, Springer, Heidelberg, 2012.
- [26] ———, *Computation of best L^∞ exponential sums for $1/x$ by Remez’ algorithm*, *Comput. Vis. Sci.*, 20 (2019), pp. 1–11.
- [27] W. HACKBUSCH AND B. N. KHOROMSKIJ, *Tensor-product approximation to operators and functions in high dimensions*, *J. Complexity*, 23 (2007), pp. 697–714.

- [28] W. HACKBUSCH AND S. KÜHN, *A new scheme for the tensor representation*, J. Fourier Anal. Appl., 15 (2009), pp. 706–722.
- [29] B. HASHEMI AND L. N. TREFETHEN, *Chebfun in three dimensions*, SIAM J. Sci. Comput., 39 (2017), pp. C341–C363.
- [30] N. J. HIGHAM, *The numerical stability of barycentric Lagrange interpolation*, IMA J. Numer. Anal., 24 (2004), pp. 547–556.
- [31] B. N. KHOROMSKIJ, *$O(d \log N)$ -quantics approximation of N -d tensors in high-dimensional numerical modeling*, Constr. Approx., 34 (2011), pp. 257–280.
- [32] A. KLIMKE, *Sparse grid interpolation toolbox v5.1.1*, 2008.
- [33] T. G. KOLDA AND B. W. BADER, *Tensor decompositions and applications*, SIAM Rev., 51 (2009), pp. 455–500.
- [34] D. KRESSNER AND L. PERIŠA, *Recompression of Hadamard products of tensors in Tucker format*, SIAM J. Sci. Comput., 39 (2017), pp. A1879–A1902.
- [35] T. H. LUU, Y. MADAY, M. GUILLO, AND P. GUÉRIN, *A new method for reconstruction of cross-sections using Tucker decomposition*, J. Comput. Phys., 345 (2017), pp. 189–206.
- [36] J. C. MASON AND D. C. HANDSCOMB, *Chebyshev polynomials*, Chapman and Hall/CRC, 2002.
- [37] H. NIEDERREITER, *Random number generation and quasi-Monte Carlo methods*, vol. 63 of CBMS-NSF Regional Conference Series in Applied Mathematics, Society for Industrial and Applied Mathematics (SIAM), Philadelphia, PA, 1992.
- [38] A. NOUY, *Low-rank methods for high-dimensional approximation and model order reduction*, in Model reduction and approximation, vol. 15 of Comput. Sci. Eng., SIAM, Philadelphia, PA, 2017, pp. 171–226.
- [39] ———, *Higher-order principal component analysis for the approximation of tensors in tree-based low-rank formats*, Numer. Math., 141 (2019), pp. 743–789.
- [40] I. OSELEDETS AND E. TYRTYSHNIKOV, *TT-cross approximation for multidimensional arrays*, Linear Algebra Appl., 432 (2010), pp. 70–88.
- [41] I. V. OSELEDETS, *Approximation of matrices with logarithmic number of parameters*, Doklady Math., 428 (2009), pp. 23–24.
- [42] ———, *Tensor-train decomposition*, SIAM J. Sci. Comput., 33 (2011), pp. 2295–2317.
- [43] R. B. PLATTE AND L. N. TREFETHEN, *Chebfun: a new kind of numerical computing*, in Progress in industrial mathematics at ECMI 2008, vol. 15 of Math. Ind., Springer, Heidelberg, 2010, pp. 69–87.
- [44] P. RAI, H. KOLLA, L. CANNADA, AND A. GORODETSKY, *Randomized functional sparse Tucker tensor for compression and fast visualization of scientific data*, arXiv e-prints, (2019), p. arXiv:1907.05884.
- [45] M. V. RAKHUBA AND I. V. OSELEDETS, *Fast multidimensional convolution in low-rank tensor formats via cross approximation*, SIAM J. Sci. Comput., 37 (2015), pp. A565–A582.
- [46] A. K. SAIBABA, *HOID: higher order interpolatory decomposition for tensors based on Tucker representation*, SIAM J. Matrix Anal. Appl., 37 (2016), pp. 1223–1249.
- [47] S. A. SAUTER AND C. SCHWAB, *Boundary element methods*, vol. 39 of Springer Series in Computational Mathematics, Springer-Verlag, Berlin, 2011. Translated and expanded from the 2004 German original.

- [48] D. SAVOSTYANOV AND I. OSELEDETS, *Fast adaptive interpolation of multi-dimensional arrays in tensor train format*, in The 2011 International Workshop on Multidimensional (nD) Systems, 2011, pp. 1–8.
- [49] R. SCHNEIDER AND A. USCHMAJEW, *Approximation rates for the hierarchical tensor format in periodic Sobolev spaces*, J. Complexity, 30 (2014), pp. 56–71.
- [50] A. M. STUART, *Inverse problems: a Bayesian perspective*, Acta Numer., 19 (2010), pp. 451–559.
- [51] A. TOWNSEND, *Computing with functions in two dimensions*, ProQuest LLC, Ann Arbor, MI, 2014. Thesis (D.Phil.)–University of Oxford (United Kingdom).
- [52] A. TOWNSEND AND L. N. TREFETHEN, *An extension of Chebfun to two dimensions*, SIAM J. Sci. Comput., 35 (2013), pp. C495–C518.
- [53] L. N. TREFETHEN, *Approximation theory and approximation practice*, Society for Industrial and Applied Mathematics (SIAM), Philadelphia, PA, 2013.
- [54] ———, *Cubature, approximation, and isotropy in the hypercube*, SIAM Rev., 59 (2017), pp. 469–491.
- [55] ———, *Multivariate polynomial approximation in the hypercube*, Proc. Amer. Math. Soc., 145 (2017), pp. 4837–4844.
- [56] L. R. TUCKER, *Some mathematical notes on three-mode factor analysis*, Psychometrika, 31 (1966), pp. 279–311.
- [57] D. XIU, *Stochastic collocation methods: a survey*, in Handbook of uncertainty quantification. Vol. 1, 2, 3, Springer, Cham, 2017, pp. 699–716.